



## 4D Traction Force Microscopy Reveals Asymmetric Cortical Forces in Migrating *Dictyostelium* Cells

H. Delanoë-Ayari\* and J. P. Rieu

*Université de Lyon, F-69000, France; Université Lyon 1, Laboratoire PMCN; CNRS, UMR 5586; F-69622 Villeurbanne Cedex, France*

M. Sano

*Department of Physics, University of Tokyo, Tokyo 113-0033, Japan*

(Received 16 December 2009; revised manuscript received 27 September 2010; published 7 December 2010)

We present a 4D ( $x; y; z; t$ ) force map of *Dictyostelium* cells crawling on a soft gel substrate. Vertical forces are of the same order as the tangential ones. The cells pull the substratum upward along the cell, medium, or substratum contact line and push it downward under the cell except for the pseudopods. We demonstrate quantitatively that the variations in the asymmetry in cortical forces correlates with the variations of the direction and speed of cell displacement.

DOI: [10.1103/PhysRevLett.105.248103](https://doi.org/10.1103/PhysRevLett.105.248103)

PACS numbers: 87.17.Jj, 87.80.Ek

For several years now, since the pioneering works of Harris *et al.* [1], forces exerted by crawling cells on elastic substrates have been measured. Different kinds of techniques were employed. A successful one proved to be flexible substrates in which fluorescent beads were incorporated. Force fields can be reconstructed from the displacements of the beads thanks to the linear theory of elasticity [2]. It has led to interesting findings concerning, for example, the link between focal adhesions and forces exerted by stress fibers [3], the role of nascent focal adhesions in the generation of propulsive forces [4], the existence of a traction stress asymmetry along the axis of polarized *Dictyostelium* cells [5,6], and was even applied on multicellular systems [7]. But, until recently, traction force microscopy was only used to measure the force component parallel to the substrate. The first reason was that parallel and perpendicular forces were supposed to be completely decoupled (assuming that the Poisson's ratio of the gel was 0.5, and that the displacement measurements of the beads was done at the cell or substrate  $z = 0$ ). However, this last condition is strictly impossible to achieve experimentally because of the finite depth of field of microscope objectives. The second reason was that, as the cells under scrutiny were mainly adhering to their substrates through "focal contacts," i.e., adhesion structures where actin-myosin structures were exerting forces parallel to the substrates, the role of the  $z$  force component was supposed to be negligible. But recently, works have shown that measurements of  $z$  forces were feasible and reveal that even in cells adhering mainly through focal contacts the  $z$  deformations existed [8,9].

In other cell types, there is even less reason to neglect the vertical forces and we indeed show that vertical forces with the same magnitude as tangential forces exist for *Dictyostelium* cells, which are amoebae moving very fast and which do not present "focal contact" like structures.

Tracking vertical deformations is trickier than tracking in-plane ones and results in a far more dense collection of data. This constitutes probably a third practical reason for which vertical forces were not measured. Even if the resolution in the  $z$  direction is smaller than in the  $xy$  directions, a subpixel resolution can be easily achieved [10] by fitting vertical fluorescent beads profiles. Nowadays, with the simple power of a desktop computer these calculations are easily accessible and we can no more ignore vertical forces. In this Letter, we will present our method to calculate the 3D force field, we will compare results with conventional 2D traction force microscopy and, finally, we will show how it is crucial to obtain a true insight in cell locomotion.

For several years now, algorithms for three-dimensional tracking have been developed [11]. But until recently, they have not been employed to study forces exerted by cells. Here we applied such techniques [12] for the measurement of forces exerted by the amoeba *Dictyostelium Discoideum*, for which we observed very important deformations of soft substrates in the  $z$  directions. Figures 1(a) and 1(b) exemplify it. In the image center of Fig. 1(a), we observe a "black" hole exactly where the cell is. Beads are out of focus because they are pushed underneath by the cell. By comparison, Fig. 1(b) shows the same field of view but without cell: all the beads are in focus. To calculate the displacement field we used the 3D particle tracking algorithm developed by Weeks and Crocker [12]. Figure 1(c) shows the in-plane projection of the displacement field obtained from the stack whose first plane is presented in Figs. 1(a) and 1(b). Displacements whose  $z$  component is negative (due to forces that push the gel down) are represented in green (light gray) and displacements whose  $z$  component is positive are represented in red (medium gray). As a comparison, we present in Fig. 1(d) the displacement field obtained by a traditional 2D particle image

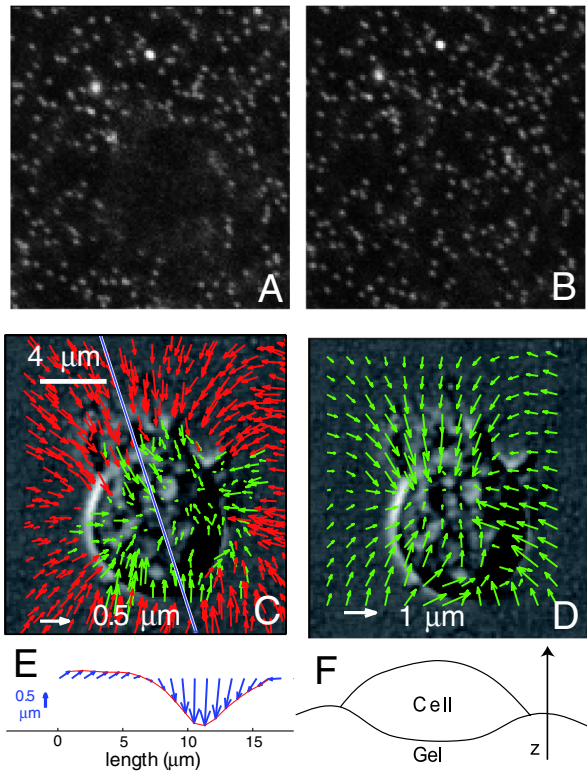


FIG. 1 (color online). (a) and (b) represent a field of fluorescent beads on the upper surface of the elastomer: (a) with a cell above and (b) without it. Note the black hole in the middle of the field (a) due to the fact that beads are pushed underneath by the cell and brought out of focus. (c) represents the measured in-plane projection of the 3D bead displacements on this particular field of view (in red [medium gray] movement of bead pointing towards the cell and in green [light gray] beads that are pushed towards the interior of the gel by the cell). (d) PIV calculation (i.e., 2D) on the same field with a window size of  $(16 \times 16)$  pixels, and a 50% overlap between windows. (e) Upper surface bead displacement in a vertical plane along the line depicted in (c). The red line depicts the upper gel surface deformation. (f) Scheme of the cell on the gel, it deforms the substrate as a droplet would do adhering on a very soft substrate.

velocimetry (PIV) algorithm [6], obtained from the first plane images of the same stack. Although, it seems difficult to measure reliable bead displacements in the inner part of the cell where beads are depleted [Fig. 1(a)], a traditional PIV algorithm will be able to furnish a smooth deformation field simply by filtering and interpolating the data. In Fig. 1(e), we present the displacements of the upper beads in the vertical plane along the blue line in Fig. 1(c). This line first crosses over a lamellipodium (top left) under which no deformation is observed, then crosses over the nucleus under which the maximum deformation is measured. Note that we obtained here a very similar push-pull pattern to the one obtained by Hur *et al.* [9] on endothelial cells. We also found this type of pattern on fibroblasts (See Supplementary Figure 3 in Ref. [12]).

From the displacement field and from the Boussinesq equation for a semi-infinite elastic medium, it is possible to use the same regularization technique as in Ref. [6] to obtain the force field exerted by the cell on the substrate [12]. Notice that for a Poisson ratio  $\nu = 0.5$ , the vertical deformation in the plane  $z = 0$ , is simply related to the vertical force as:  $u_z(r) = \int dr' G_{zz}(r - r') F_z(r')$  [2]. We present in Fig. 2(a) the in-plane projection of the force field obtained from the displacement field of Fig. 1(c), and a force profile along the blue line [Fig. 2(c)]. As a comparison, we present the 2D force field obtained from the 2D PIV displacement field [Fig. 2(b)]. Two main differences can be seen. The magnitude of forces in the case of the purely 2D reconstruction is slightly higher; this is very reasonable as in-plane displacements due to the ignored  $z$  forces have to be compensated by overestimated in-plane forces. One other striking feature is the fact that forces are much more “spread” under the cell in the 2D case, whereas in the 3D case, forces are much better localized on the cell contour: the solution is “over-regularized” due to the absence of exact solution in 2D. We can separate peripheral forces with a  $z$  component oriented upward from inner forces whose  $z$  component is oriented downward. The origin of the upward peripheral forces is easily attributed to the cortical tension exerted by the membrane on the side of the cell through adhesion points to the substrate. As the sum of forces in the  $z$  direction has to be zero, forces

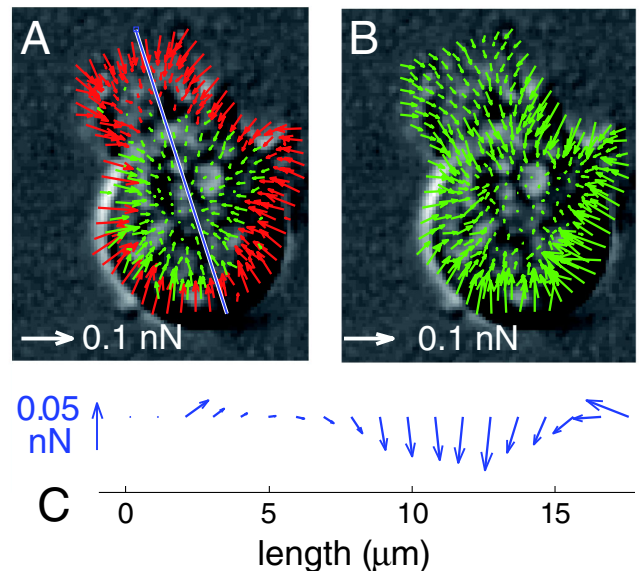


FIG. 2 (color online). (a) In-plane projection of the 3D forces calculated from the displacement vectors of Fig. 1(c). The same color convention as in Fig. 1(c) is used (in red [medium gray] forces pointed towards the cell and in green [light gray] forces pointed toward the gel). (b) 2D forces calculated with the PIV displacements of Fig. 1(d). (c) Force profile along the blue line drawn in (a).

pushing the gel downward have to compensate for these upwards forces: they originate probably from the nucleus pushing downwards as compressed by the rigid cortex. This is very well in agreement with recent observations showing that the nucleus can be strongly deformed when a cell adheres on a rigid and micropatterned surface [13]. Here, substrates are softer than the nucleus (the elastic modulus of the nucleus is of the order of 1–5 kPa, i.e., 2 to 10 times larger than the elastomer elastic modulus [14]), the substrate is therefore deformed but not the nucleus. Moreover, it corroborates the fact that no  $z$  deformation is observed under the lamellipodium [see Fig. 1(e)].

All in all, the force pattern exposed here reminds us of the force pattern of a drop adhering on a surface and exerting forces on it through its surface tension. However, one key feature which has been observed on liquids seems to be missing here: the sharp rising edge around the drop, where the surface tension is pulling up the substrate [12]. We only observe a bump [See Fig. 1(e)]. But this can be easily explained, as in the case of the drop the surface tension  $\gamma$  times the perimeter  $L \sim 2\pi R$  ( $R$  is the radius of the drop on the surface) has to be compensated by the hydrostatic pressure  $P$  times the projected area  $A \sim \pi R^2$ . In the case of the cell, if the cortical tension is balanced by the pressure exerted by the nucleus which has a much smaller area than the cell, the ratio of cortical to pressure is much lower than in the case of a liquid drop. As a consequence, the rise on the edge will be much smaller.

We now analyze the time series of 3D traction forces. We have followed several *Dictyostelium* cells during their random motion on flexible substrata, and have calculated forces exerted by the cell during 50 frames separated by 8.5 sec each. Our first result is that the radial and the vertical stress components, (i.e.,  $\sigma_t$  and  $\sigma_n$  defined, respectively, as the sum of the absolute values of in-plane projections and as the sum of the vertical components of the same peripheral forces, both divided by the cell perimeter) are proportional (Fig. 3). We can fit the data by a straight line with a slope of 0.72. This measurement would in principle permit us to calculate the in-plane cortical tension  $\sigma_1$  and compare it to  $\sigma_2$ , the one exerted along the membrane going off the substrate (see inset of Fig. 3), provided that the contact angle is known. It would be very interesting in the future to find a technique which would give access to this parameter. Reflection interference contrast microscopy [15] is not usable because of the thick (i.e., about 70  $\mu\text{m}$ ) gel substrate but reconstruction techniques from stacks may be helpful [16]. We can, however, make a simple assumption as to get an estimate of the cell surface tension, stating that there is only a cortical tension in the upper surface  $\sigma_1 = 0$ . This leads us to  $\theta \approx 36^\circ$  and gives us a typical value of 0.1  $\text{nN}/\mu\text{m}$ . This is low compared to some recent estimations [17] on endothelial cells, but in good agreement with other values found in the literature [18] on the same type of cells.

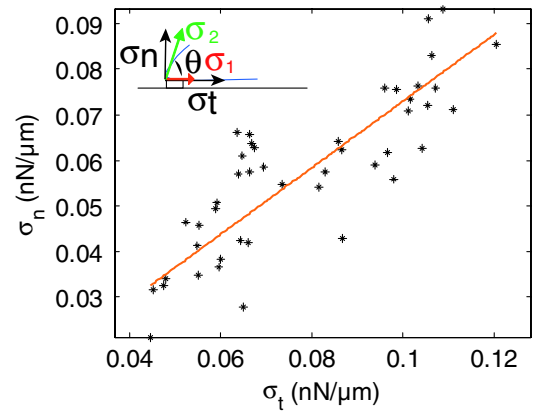


FIG. 3 (color online). Radial stress  $\sigma_t$  is proportional to normal stress  $\sigma_n$ . The orange line is a linear fit of the data going through zero. The slope is 0.72. The inset on the left top is a scheme of the different membrane tensions acting on the membrane on the edge of the cell.  $\sigma_1$  is the in-plane tension.  $\sigma_2$  is the tension in the membrane going off the substrate.  $\theta$  is the angle between the two membranes.

Another important result obtained from our measurements is that, for the first time for amoeboid cells, a clear correlation between cell speed and forces variations is revealed. Different authors proposed that one key point to understanding amoeboid cell movement was the asymmetry of the tension between the front and the back of the cell on the cell contour [5]. However, such an asymmetry was not parameterized and no correlation with cell speed was plotted. Here, we have considered the total peripheral in-plane traction forces projected on the cell speed axis. This parameter is null if the cell is perfectly symmetric. Otherwise it is balanced by inner in-plane forces. As a function of time, the in-plane force asymmetry exhibits a periodic behavior as does the cell speed. Such a periodic behavior is well known for *Dictyostelium* cells. Cell speed oscillates with a 1–2 min period both in the vegetative [19] and aggregating phase [16]. This periodicity is due to an extension-retraction cycle that has a 3D component (cyclic  $z$ -axis extension). Figure 4 shows that there is a clear correlation between cell speed changes and the ones of

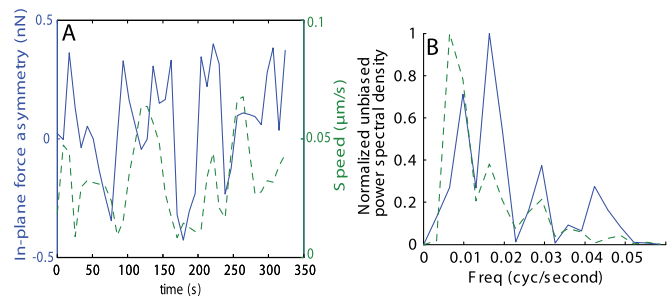


FIG. 4 (color online). (a) Temporal variations of the in-plane force asymmetry compared to temporal variations of the cell speed. (b) Unbiased power spectral density of the same data.

in-plane peripheral force asymmetry. There is no direct linear correlation between the two quantities; however, the variations are very well correlated, as demonstrated by the unbiased power spectral densities which present the same peaks in the two signals [Fig. 4(b)].

If cell movement is associated with a spatial asymmetry in cortical tension, we propose that the unbalance in in-plane forces between the front and the back of the cell has to be compensated by forces arising from actin polymerization. If the cell was not linked to a substrate this competition between the cortex and the polymerization could lead to oscillation of the shape of the cell, but would never lead to a net cell movement. These forces have to be transmitted to the substrate. It is now well known that actin polymerization often entails a retrograde flux of actin along the substratum, leading to a relative speed of the interior of the cell with respect to the substrate. Several studies on distinct systems have shown that the retrograde flow speed is anticorrelated with cell speed [20]. Moreover, it was proposed a while ago [21] that force transmission of actin polymerization to the substratum is due to a molecular clutch of proteins. The more the clutch is engaged the smaller the retrograde flow and the higher the speed and the higher the force on the substratum [22]. This hypothesis is fully compatible with our results. It would be very interesting in future studies to test this and to identify these molecular clutches, if they exist. Have they something to do with actin foci [23], which are adhesive structures identified in *Dictyostelium*?

In summary, we have shown in this Letter that, taking into account forces in the  $z$  direction is of the most importance for cells such as *Dictyostelium* that notably exhibit large vertical deformations. First, it enables us to obtain much more accurate in-plane traction force measurements, because it avoids over-regularizing the in-plane force solution. Second, it enables the localization and the quantification of cortical forces and gives new information on perpendicular forces. We were able to show a relation between forces exerted by the actin polymerization process and the speed of the cell. We have applied this technique to the amoeba *Dictyostelium discoideum*, but it is also possible to measure  $z$  forces exerted by regular fibroblast on substrata with a very good spatial resolution as exemplified in Supplementary Figure 3 in Ref. [12]. We believe the

application of this technique will lead the scientific community to new interesting features and that it cannot be ignored anymore.

H. D.-A. and J. P. R. belong to the CNRS consortium CellTiss. J. P. R. acknowledges support from Center for Interdisciplinary Research (CIR, Tohoku University). We thank S. Iwaya and C. Rivière for helping us in data collection. We deeply acknowledge people who freely make available their code on the web.

---

\*helene.ayari@univ-lyon1.fr

- [1] A. K. Harris, P. Wild, and D. Stopak, *Science* **208**, 177 (1980).
- [2] M. Dembo and Y. L. Wang, *Biophys. J.* **76**, 2307 (1999).
- [3] N. Q. Balaban *et al.*, *Nat. Cell Biol.* **3**, 466 (2001).
- [4] K. A. Beningo *et al.*, *J. Cell Biol.* **153**, 881 (2001).
- [5] M. L. Lombardi *et al.*, *J. Cell Sci.* **120**, 1624 (2007).
- [6] H. Delanoë-Ayari *et al.*, *Cell Motil. Cytoskeleton* **65**, 314 (2008).
- [7] X. Trepate *et al.*, *Nature Phys.* **5**, 426 (2009).
- [8] S. A. Maskarinec *et al.*, *Proc. Natl. Acad. Sci. U.S.A.* **106**, 22108 (2009).
- [9] S. S. Hur *et al.*, *Cell. Mol. Bioeng.* **2**, 425 (2009).
- [10] Y. Gao and M. L. Kilfoil, *Opt. Express* **17**, 4685 (2009).
- [11] E. Weeks *et al.*, *Science* **287**, 627 (2000).
- [12] See supplementary material at <http://link.aps.org/supplemental/10.1103/PhysRevLett.105.248103> for a detailed description of material and methods, tests of the methods, and for supplementary figures.
- [13] P. Davidson *et al.*, *Adv. Mater.* **21**, 3586 (2009).
- [14] N. Caille *et al.*, *J. Biomech.* **35**, 177 (2002).
- [15] R. Simson *et al.*, *Biophys. J.* **74**, 514 (1998).
- [16] D. Wessels *et al.*, *Cell Motil. Cytoskeleton* **41**, 225 (1998).
- [17] I. B. Bischofs, S. S. Schmidt, and U. S. Schwarz, *Phys. Rev. Lett.* **103**, 048101 (2009).
- [18] H. Delanoë-Ayari *et al.*, *Phys. Rev. Lett.* **93**, 108102 (2004).
- [19] D. R. Soll, *Computerized Medical Imaging and Graphics* **23**, 3 (1999).
- [20] C. Jurado *et al.*, *Mol. Biol. Cell* **16**, 507 (2004).
- [21] T. Mitchison and M. Kirschner, *Neuron* **1**, 761 (1988).
- [22] L. Bard *et al.*, *J. Neurosci.* **28**, 5879 (2008).
- [23] K. S. K. Uchida and S. Yumura, *J. Cell Sci.* **117**, 1443 (2004).